Hydrothermal Deposition of Bioresorbable Coating on AZ31 Magnesium for Implant Application

S. Kaabi[1, 2] , S. Nemeth[1], M.J.Tan[2]

Abstract

Interest in biodegradable magnesium (Mg) implants has increased dramatically in the last decade due to their desirable mechanical properties that are close to that of human bone, thus avoiding stress shielding effect. In addition, Mg is resorbed in the body and surgery to remove the implant after healing is not needed. However, the high corrosion rate of magnesium and its alloys severely limit their practical applications as implants. To control the corrosion rate of magnesium, biocompatible and bioresorbable Ca-P (calcium phosphate) coatings were deposited in this study using AZ31 magnesium substrate and hydrothermal deposition process. Coatings obtained at various temperatures were found to mainly consist of a mixture of monetite [$CaHPO_4$] and tricalcium phosphate [$Ca_{2.86}Mg_{0.14}(PO_4)_2$] with partially magnesium substituted tricalcium phosphate structure as determined by XRD (X-ray diffraction) and FTIR (Fourier transform infrared) spectroscopy methods. Coating morphology was examined with scanning electron microscopy (SEM) and the results showed that coatings became denser with increasing temperature. Coating adhesion was examined by pull-out adhesion test indicating only coating cohesive failure at 5.2-5.8 MPa. It was clearly observed that significant portion of the coating still remained on the substrate after adhesion test. Potentiodynamic polarization conducted in SBF (simulated body fluid) solution confirmed that coating significantly enhanced the corrosion performance of Mg substrate. The corrosion current density of Mg substrate decreased approximately 10,000-fold in the presence of coating. The mass loss for the coated samples was only around 1/3 of that observed for bare substrate, and the amount of Mg ions released from the coated samples was significantly lower than in case of bare substrate after immersion in SBF solution. The described hydrothermal method provided crystalline and compact coatings with excellent adhesion strength and significantly improved corrosion resistance with good prospects for biomedical application.

Keywords: Magnesium, Hydroxyapatite coating, Corrosion resistance

1 BACKGROUND

Stainless steel, titanium and cobalt-based alloys, as well as various ceramic materials are commonly used for implants to support fractured human bones. However, due to mismatches in mechanical properties between the implants and bones, stress shielding effect is present, and release of poisonous ions by corrosion or mechanical wear is a danger. Additionally, a second surgery is frequently needed to remove the implant after healing is complete [1-4].

Metallic biodegradable implant material is desirable in cases when no further support is needed after bone healing. Recently, magnesium alloys have attracted significant interest as biodegradable implant materials due to their excellent properties. Magnesium plays a major part in metabolism and can dissolves completely in body environment. Therefore, the need for a second operation after bone healing to remove the implant is eliminated. Since the mechanical properties of magnesium are closer to that of bone than conventional implant materials the stress shielding effect could be avoided or minimised as well [5-7].

The ions released due to the corrosion of magnesium in the body can be absorbed in the tissues or eliminated over time. The dissolution of magnesium implants also decreases the chance of an immune response [4-9]. The decrease in immune response is due to the continuous formation of fresh interface between the living tissue and implant as the surface dissolves, thus reducing the chance of sheltering bacteria and other microorganisms at the non-living material surface where the immune system may have limited access. However, the high degradation rate of magnesium alloys is the major reason that limits or even prevents their large-scale use, resulting in rather rapid loss of mechanical integrity in human body environments [2, 7]. Hence, enhancing the corrosion resistance of magnesium alloys and preventing the quick loss of their strength is an outstanding challenge that can lead to more widespread biomedical applications and possibly other industrial uses[8, 10]. In case of biomedical applications, a relatively modest ex-

[1] Singapore Institute of Manufacturing Technology, Singapore

[2] Nanyang Technological University , School of Mechanical & Aerospace Engineering, Singapore

tension of implant lifetime of two to ten-fold improvement is sufficient. When using temporary implants, full healing usually takes place in less than a year. Thus, extending the lifetime of the implant for up to one year in the body is adequate.

During the last decades of research, a number of methods were developed for the deposition of HA (hydroxyapatite) coatings on metallic implants, including: electrodeposition [11, 12], sol-gel coating [13], and biomimetic methods [14]. these coatings could potentially offer protection to the Mg alloy substrate; however, in the case of biomimetic method coatings are extremely permeable, and exhibit many cracks[15] or in the electrodeposition method, the release of hydrogen bubble on the Mg surface creates imperfections in the coating, resulting in poorly adherent and non-uniform layer. The hydrogen bubbles adhere to the surface and impede the nucleation and deposition of coating [12, 16]. In order to further improve the corrosion protection, a new hydrothermal method is presented in this work for producing dense and adherent coatings over a large surface area suitable even for irregular geometry. The deposition of Ca-P coating accelerates under hydrothermal conditions and thick, dense coatings can be formed. Deposition of Ca-P ceramic coating on the surface of AZ31 alloy, the analysis of the coating properties, and its corrosion protection is discussed in the present paper.

2 METHODOLOGY

2.1 Experimental Procedures

Analytical grade $Ca(NO_3)_2$ (99.98% purity) and $NH_4H_2PO_4$ (98% purity) were obtained from Alfa Aesar. AZ31 magnesium alloy was used as substrate for the coating process. Disks were prepared with 25 mm diameter and 2 mm thickness using commercial AZ31 rod. Prior to coating process, AZ31 substrate was abraded with up to 2400 grit abrasive paper, and then ultrasonically cleaned in acetone for 20 minutes. In order to deposit Ca-P coating on the Mg substrate; hydrothermal process was used. A solution of $Ca(NO_3)_2$ (0.1M) and $NH_4H_2PO_4$ (0.06 M) was prepared for the process. The pH of solution was adjusted to 3.9-4.0 by using ammonia. The AZ31 samples and deposition solution were placed in a stainless steel autoclave with polytetrafluoroethylene lining and heated in an electric oven at different temperatures (100 ºC, 130 ºC, 160 ºC and 190 ºC) for 3 hours. *Warning:* magnesium may generate hydrogen gas in aqueous environment that could increase the pressure significantly and allowance must be made for such potential pressure rise to safely conduct the hydrothermal process.

The samples were named as HE100 ºC-3hr, HE130 ºC-3hr, HE160 ºC-3hr and HE190 ºC-3hr according to the respective deposition temperature and time.

2.2 Coating Characterization

The surface phase of the coated samples was characterized by X-ray diffractometer (XRD, Panalytical Empyrean, DY2t), using Cu-Kα1 radiation (wavelength λ= 1.5406Å). The surface morphology and the chemical composition were analyzed using scanning electron microscope (JEOL JSM 5600 SEM) with an EDS (INCA system, Oxford Instruments, UK).

FTIR (VERTEX 80V) measurements were carried out to verify the deposition of Ca-P coatings. First, the coating layer was carefully scraped from the AZ31 substrate, and then mixed with potassium bromide (KBr) powder in 1:50 weight ratio, and then the mixtures were compressed into a disc for characterization. Analyses were performed in the 400 to 4000 cm^{-1} wave number range.

The electrochemical behaviour of uncoated and coated samples was investigated by potentiodynamic polarization tests conducted in simulated body fluid (SBF) [18] solution at pH 7.2. A three-electrode cell was used with the sample as working electrode, Hg_2Cl_2/Hg/ (sat. KCl) as the reference, and graphite as the counter electrode. An area of 1 cm^2 of the working electrode was exposed to the solution. A 1 mV s^{-1} scanning rate was applied during the potentiodynamic polarization test. Prior to the polarization test, samples were stabilized in SBF for 30 min. The SBF solution was exposed to air and was saturated with the respective components of air.

The immersion tests were conducted in the SBF standard solution for up to 28 days in order to assess the early corrosion performance of the coated and uncoated substrate. Each sample with an exposure area of 4.9 cm^2 was immersed in 50 ml of the SBF solution at 37 ºC. After each immersion period in SBF solution, 5 ml of solution was extracted and analyzed by using an inductively coupled plasma atomic emission spectrometer (ICP-MS7700, Agilent) in order to determine the Mg ions release from the samples during the immersion's periods. The change in pH value of the SBF solution for uncoated and coated specimens was monitored at different time periods as well. Adhesion strength between coating layer and AZ31 substrate was evaluated based on ISO 13779-4. Pull-out test was carried out by using Instron testing machine at a cross head speed of 1 mm/min and.

3. RESULTS & DISCUSSION

By increasing the temperature, calcium/phosphate salt solubility decreased and consequently the solution became supersaturated resulting in Ca-P mineral deposition on the surface of Mg substrate. At pH below 5, biocompatible and bioresorptive monetite and calcium pyrophosphate are the most stable phosphate phases. However, the presence of Mg ions

can stabilize the tricalcium phosphate phase. The stabilizing effect of Mg is attributable to the markedly smaller ionic radius of Mg^{2+} (0.65 Å) compared to Ca^{2+} (0.99 Å)[17]. The XRD analysis indeed showed that coated materials obtained from the hydrothermal process were a mixture of monetite ($CaHPO_4$), tricalcium phosphate, and calcium pyrophosphate ($Ca_2P_2O_7$) as shown in Figure 1.

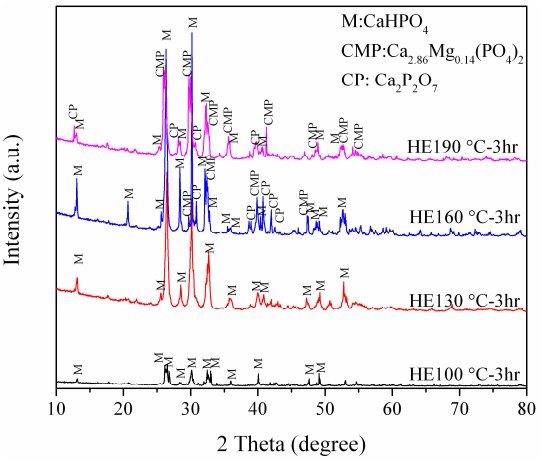

Fig.1. XRD pattern of coatings on AZ31 at different deposition temperatures

Figure 2 shows the morphology of Ca-P coating obtained from the hydrothermal process. The coating morphologies are compact, pore free, and clearly show triclinic structure. The coated sample at 100 ºC displayed a plate like morphology. By increasing the deposition temperature, the gap size between crystals decreased and the coating became denser. Additionally, the amount of deposited Ca-P and the size of crystals increased significantly. The solubility of Ca-P decreases with increasing the temperature; consequently, a higher amount of Ca-P is deposited on the substrate. Moreover, diffusion rate increases by increasing the deposition temperature; hence, the reactants move to the substrate more easily. During the initial phase of the hydrothermal process, the deposition solution (pH: 3.9-4.0) etches the Mg substrate and forms a rough metal surface with pits. The etched pits in the surface of Mg substrate may act as nucleation sites for Ca-P deposition and growth [18].

The FTIR spectra for Ca-P coating layers deposited at different temperatures are given in Figure 3 showing all the vibration bands that correspond to P-O stretching, P-O(H) stretching, O-P-O(H) and O-P-O in the range of 400-1400 cm^{-1}. These bands are characteristics for monetite structure [19, 20]. The peaks at 548 cm^{-1} and 603 cm^{-1} correspond to the PO_4^{3-} band in tricalcium phosphate structure. The observed bands were in general agreement with literature [21, 22].

The potentiodynamic curves for uncoated and Ca-P coated AZ31 samples in SBF solution are shown in Figure 4.The electrochemical studies in SBF solution revealed that coated samples exhibit higher corrosion resistance compared to uncoated samples.

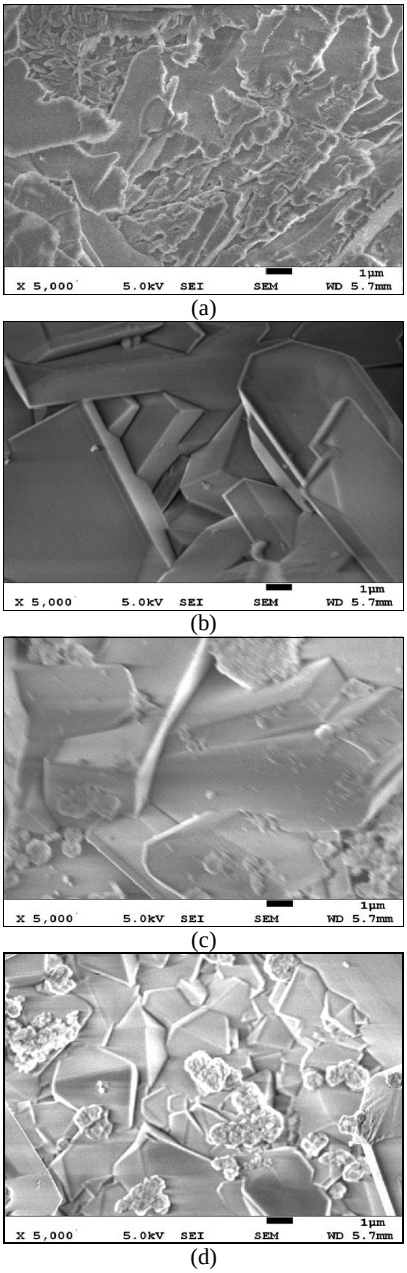

Fig.2. SEM micrograph of coated AZ31 (a) 100 ºC, (b) 130 ºC, (c) 160 ºC and (d) 190 ºC. In all cases, the deposition time was 3 hours

The corrosion tendency of the samples were characterised by the corrosion current density and the corrosion potential. The corrosion current, i_{corr}, was determined by the Tafel extrapolation method from the potentiodynamic polarisation curves.

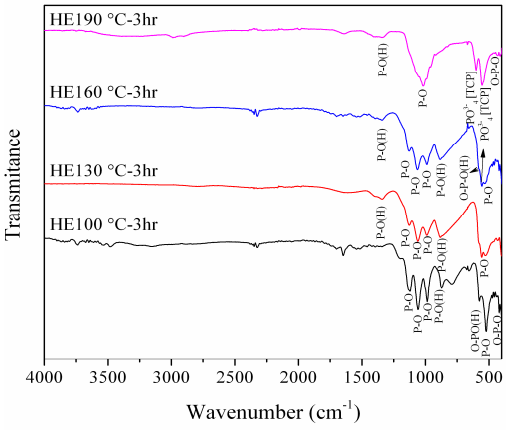

Fig.3. FTIR spectrum of coated AZ31

The corrosion resistance of Mg substrate was enhanced 10,000-fold with coating deposited at 190 ºC. Mg and its alloys tend to suffer from localized corrosion with characteristic rapid increase in the anodic current over small polarization potential range and this is clearly seen in Figure 4 for the bare substrate and sample coated at 100 ºC. In the case of samples coated at 130 ºC and 160 ºC, polarization curves show an abrupt increase in anodic current followed by a quasi-passive region at around 10^{-5} Acm^{-2}. While in the case of sample coated at 190 ºC, a quasi-passive region in the polarization curve was at around $5*10^{-7}$ Acm^{-2}. The corrosion potential (E_{corr}) of the coated samples was shifted to the nobler potential. The positive shift of E_{corr} indicates the formation of a stable Ca-P/AZ31 interface. The nobler behaviour of the coated sample at 190 ºC might be attributed to the stable behaviour of the coated surface.

By increasing the deposition temperature, the protective nature of coating increased due to the increase in coating thickness and formation of compact morphology.

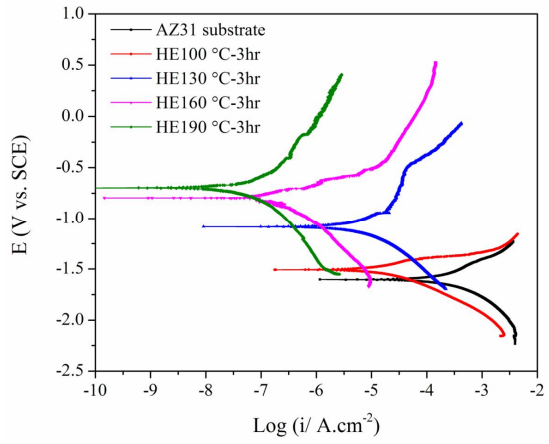

Fig.4. potentiodynamic polarization curves of the coated AZ31 samples tested in SBF

The degradation rate of Mg and its alloys in the initial stages of implantation would play a significant role in the newly formed tissue response. If the early degradation rate of Mg-based implants is too rapid, osteolysis reaction may take place; consequently, negatively affecting bone tissue regeneration and healing [23]. Figure 5 shows the mass loss for uncoated AZ31 substrate and Ca-P coated samples. The mass loss of samples were measured during the immersion period. The total mass lost from the uncoated AZ31 was approximately 38.7 mg/cm^2 after 28 days immersion in SBF solution. For the sample coated at 160 ºC the total mass loss was 14.3 mg/cm^2 after 28 days. In the case of coated samples at 130 ºC and 100 ºC the mass loss after 28 days was 21.8 mg/cm^2 and 27.6 mg/cm^2, respectively.

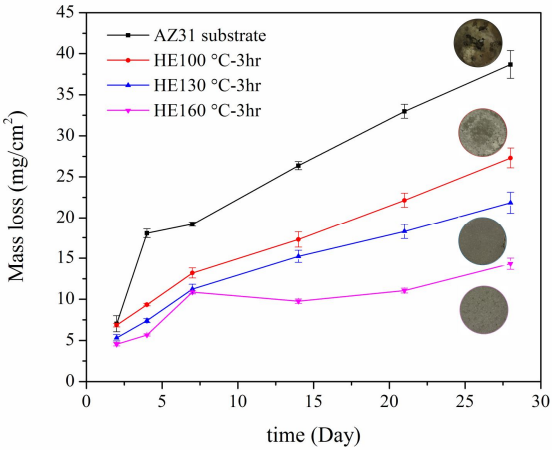

Fig.5. Mass loss for uncoated AZ31 and coated samples as a function of immersion time

The ion release of uncoated and coated samples was measured by means of ICP technique. The results are given in Figure 6 and the detailed results are summarized in Table 1. For the uncoated samples, the Mg ion release increased from 82 ppm/cm^2 after 2 days immersion to 174 ppm/cm^2 after 28 days immersion in SBF solution. The release of Mg ion from the coated sample was low compared to the uncoated sample. In the case of samples coated at 160 ºC Mg ion release starting from 11 ppm/cm^2 after 2 days immersion and reaching 107 ppm/cm^2 after 28days immersion in SBF solution. The results showed Ca-P coating can protect Mg substrate from corrosion and decrease the degradation rate of Mg substrate.

The coating thickness was measured by eddy current probe and checked with cross sectioning method shown in Figure 7. The coating thickness increased gradually from 20 µm for the sample coated at 100 ºC to around 61 µm for the sample coated at 160 ºC followed by a sharp increase to 400 µm for sample coated at 190 ºC.

Table1. Mg ion concentration released from the coated and bare substrate

Immersion period (Day)	Mg ion release (ppm/cm^2)			
	AZ31	HE100 ℃	HE130 ℃	HE160 ℃
2	82	16.6	12.8	11.2
4	102	34.7	27. 6	22.5
7	115	38.9	35.9	32.8
14	119	116	110	82
21	153	129	118	98
28	174	141	122	107

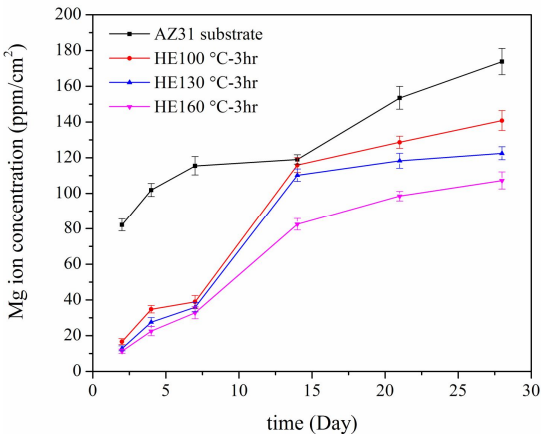

Fig.6. Mg ion release as a function of immersion time

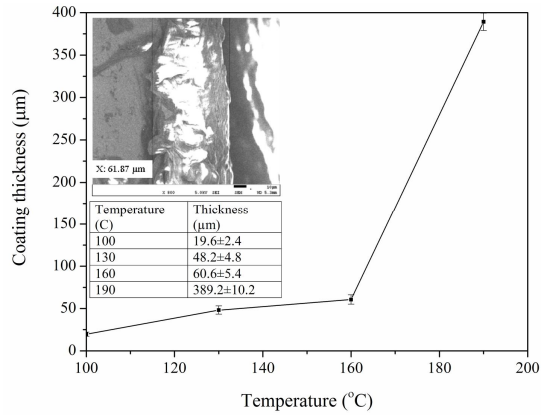

Fig.7. Coating thickness as a function of deposition temperature

The stress-displacement curves obtained from pull-out adhesion tests and coating morphology after adhesion test are shown in Figure 8. For the samples prepared at 100 ºC, 130 ºC and 160 ºC, the coatings failed by cohesive failure at around 5.2-5.8 MPa. At preparation temperature of 190 ºC, the coated sample failed at around 3.1 MPa, probably due to the increase in coating thickness and increasing the residual stress in the coating layer. The SEM micrograph of coating after pull of test clearly showed that coating still remained on the substrate.

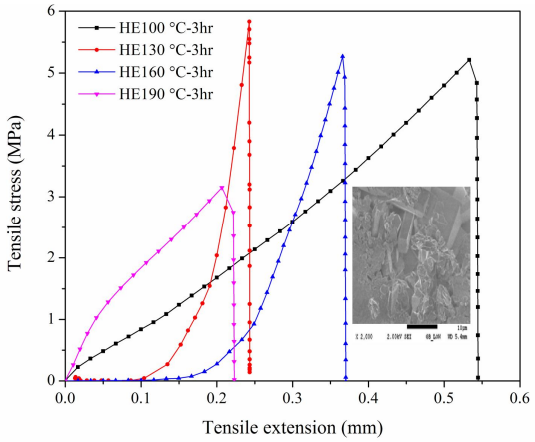

Fig.8. Coatings adhesion to the substrate

4. CONCLUSION

Dense calcium phosphate (Ca-P) coatings were successfully deposited on the Mg substrate by the hydrothermal method at different temperatures. The obtained coatings were a mixture of bioactive and resorbable monetite and tricalcium phosphate phases, as confirmed by means of XRD and FTIR techniques.

The corrosion performance of Mg substrate significantly improved after Ca-P deposition. The degradation rate of Mg substrate decreased with increasing the deposition temperature and the corrosion resistance of Mg was increased 10,000-fold. The significant increase in corrosion resistance with increase in deposition temperature might be due to an increase in coating thickness with increasing temperature.

REFERENCES

1. Witte, F., *The history of biodegradable magnesium implants: a review.* Acta Biomater, 2010. **6**(5): p. 1680-92.

2. Witte, F., et al., *Biodegradable magnesium-hydroxyapatite metal matrix composites.* Biomaterials, 2007. **28**(13): p. 2163-74.

3. Witte, F., et al., *Degradable biomaterials based on magnesium corrosion.* Current Opinion in Solid State and Materials Science, 2008. **12**(5-6): p. 63-72.

4. Zeng, R., et al., *Progress and Challenge for Magnesium Alloys as Biomaterials.* Advanced Engineering Materials, 2008. **10**(8): p. B3-B14.

5. Hornberger, H., S. Virtanen, and A.R. Boccaccini, *Biomedical coatings on magnesium alloys - a review.* Acta Biomater, 2012. **8**(7): p. 2442-55.

6. Salahshoor, M. and Y. Guo, *Biodegradable Orthopedic Magnesium-Calcium (MgCa) Alloys, Processing, and Corrosion Performance.* Materials, 2012. **5**(12): p. 135-155.

7. Salunke, P., V. Shanov, and F. Witte, *High purity biodegradable magnesium coating for implant application.* Materials Science and Engineering: B, 2011. **176**(20): p. 1711-1717.

8. Song, G. and S. Song, *A Possible Biodegradable Magnesium Implant Material.* Advanced Engineering Materials, 2007. **9**(4): p. 298-302.

9. Xu, L. and A. Yamamoto, *Characteristics and cytocompatibility of biodegradable polymer film on magnesium by spin coating.* Colloids Surf B Biointerfaces, 2012. **93**: p. 67-74.

10. Song, G., *Control of biodegradation of biocompatable magnesium alloys.* Corrosion Science, 2007. **49**(4): p. 1696-1701.

11. Lin, D.-Y. and X.-X. Wang, *Preparation of hydroxyapatite coating on smooth implant surface by electrodeposition.* Ceramics International, 2011. **37**(1): p. 403-406.

12. Song, Y.W., D.Y. Shan, and E.H. Han, *Electrodeposition of hydroxyapatite coating on AZ91D magnesium alloy for biomaterial application.* Materials Letters, 2008. **62**(17–18): p. 3276-3279.

13. Kim, H.W., et al., *Sol-gel derived fluor-hydroxyapatite biocoatings on zirconia substrate.* Biomaterials, 2004. **25**(15): p. 2919-26.

14. Keim, S., et al., *Control of magnesium corrosion and biocompatibility with biomimetic coatings.* J Biomed Mater Res B Appl Biomater, 2011. **96**(1): p. 84-90.

15. Shadanbaz, S. and G.J. Dias, *Calcium phosphate coatings on magnesium alloys for biomedical applications: A review.* Acta Biomater., 2012. **8**(1): p. 20-30.

16. Hornberger, H., S. Virtanen, and A.R. Boccaccini, *Biomedical coatings on magnesium alloys – A review.* Acta Biomater., 2012. **8**(7): p. 2442-2455.

17. Salimi, M.H., J.C. Heughebaert, and G.H. Nancollas, *Crystal growth of calcium phosphates in the presence of magnesium ions.* Langmuir, 1985. **1**(1): p. 119-122.

18. Liu, D., K. Savino, and M.Z. Yates, *Coating of hydroxyapatite films on metal substrates by seeded hydrothermal deposition.* Surface and Coatings Technology, 2011. **205**(16): p. 3975-3986.

19. Tortet, L., et al., *Study of Protonic Mobility in $CaHPO_4{\cdot}2H_2O$ (Brushite) and $CaHPO_4$(Monetite) by Infrared Spectroscopy and Neutron Scattering.* Journal of Solid State Chemistry, 1997. **132**(1): p. 6-16.

20. Xu, J., I.S. Butler, and D.F.R. Gilson, *FT-Raman and high-pressure infrared spectroscopic studies of dicalcium phosphate dihydrate (CaHPO4·2H2O) and anhydrous dicalcium phosphate (CaHPO4).* Spectrochimica Acta Part A: Molecular and Biomolecular Spectroscopy, 1999. **55**(14): p. 2801-2809.

21. Chen, J., et al., *A simple sol-gel technique for synthesis of nanostructured hydroxyapatite, tricalcium phosphate and biphasic powders.* Materials Letters, 2011. **65**(12): p. 1923-1926.

22. Tonković, M., M. Sikirić, and V. Babić-Ivančić, *Controversy about β-tricalcium phosphate.* Colloids and Surfaces A: Physicochemical and Engineering Aspects, 2000. **170**(2–3): p. 107-112.

23. Lu, W., et al., *Microstructure, Corrosion Resistance and Biocompatibility of Biomimetic HA-Based Ca-P Coatings on ZK60 Magnesium Alloy.* International Journal of Electrochemical science, 2012. **7**: p. 12668 - 12679.